ELSEVIER

Earth and Planetary Science Letters 190 (2001) 153–165

EPSL

www.elsevier.com/locate/epsl

Systematics of xenocrystic contamination: preservation of discrete feldspar populations at McCullough Pass Caldera revealed by $^{40}Ar/^{39}Ar$ dating

Terry L. Spell *, Eugene I. Smith, Aaron Sanford, Kathleen A. Zanetti

University of Nevada Las Vegas, Department of Geoscience, 4505 Maryland Parkway, Las Vegas, NV 89154-4010, USA

Received 9 November 2000; received in revised form 23 May 2001; accepted 23 May 2001

Abstract

Single crystal $^{40}Ar/^{39}Ar$ dating of K-feldspars from silicic volcanic rocks containing xenocrysts often yields a spectrum of ages slightly older than those of juvenile sanidine phenocrysts. In contrast, feldspars from thin, low-volume units of the Tertiary (14 Ma) McCullough Pass Tuff define discrete age populations at ~14 Ma, ~15 Ma, and ~1.3 Ga, reflecting the time of eruption, xenocrysts from an older ignimbrite exposed in the caldera wall, and Proterozoic basement K-feldspars, respectively. Conductive cooling and diffusion modelling suggests preservation of such discrete populations is likely only when xenocrystic material is incorporated into the magma very near or at the surface, or is engulfed in thin, rapidly cooled pyroclastic flows during emplacement. Incorporation of xenocrysts into the subvolcanic magma chamber, into thick rhyolite domes or lava flows, or into large, welded ignimbrite sheets will result in partial or total resetting of the K/Ar isotopic system. Similarly, petrographic evidence such as exsolution lamellae may be homogenized under these conditions but not in thin ignimbrites. Extremely low diffusion rates for disordering of the Al–Si tetrahedral siting of basement feldspars suggests that they will retain their ordered structural state given rhyolitic magma temperatures. Thus, even when petrographic and K/Ar isotopic evidence for xenocrystic contamination is obscured, it may be preserved in the form of Al–Si ordering.

Keywords: Ar-40/Ar-39; absolute age; xenocrysts; contamination; acidic composition; volcanic rocks

1. Introduction

Silicic volcanic systems produce a range of lithologies from explosively erupted rhyolitic ignimbrites representing >1000 km^3 of magma to effusively erupted, small volume (<1 km^3) lava flows and domes. Determining accurate and precise ages for these rocks is important for studies such as volcanic hazards, igneous petrogenesis, structural geology, fossil ages, and regional stratigraphy. The problem which xenocrystic contamination presents to dating silicic volcanic rocks is avoided by the laser fusion $^{40}Ar/^{39}Ar$ technique in which individual crystals are dated, thus allowing direct identification of xenocrysts and accurate determination of eruptive ages defined by juvenile phenocryst populations. This method is especially valuable for pyroclastic rocks as it is often not feasible to separate sanidine from pumice lapilli

* Corresponding author. Tel.: +1-702-895-1171 (office), +1-702-895-2353 (lab); Fax: +1-702-895-4064.
E-mail address: tspell@ccmail.nevada.edu (T.L. Spell).

0012-821X/01/$ – see front matter
PII: S0012-821X(01)00382-X

in welded tuff, or from tuffs poor in pumice. In these cases a whole-rock sample must be processed, increasing the probability of sampling contaminated material.

Many rhyolites show no K/Ar isotopic evidence for xenocrystic contamination, even when an extreme contrast in age exists between volcanism and basement rocks (e.g., [1]), or only minor contamination in which xenocryst ages are scattered and slightly older than juvenile phenocrysts (e.g., [2]). Less common are samples which contain significant xenocryst populations with large contrasts in age [3] or distinct age populations [4].

McCullough Pass Caldera (MPC) Tuffs preserve xenocryst populations of distinct age, one of which is substantially older than the eruptive age. Based on diffusion parameters for K-feldspar and conductive cooling models for lava flows and ignimbrites we suggest that most xenocrystic contamination detectable by $^{40}Ar/^{39}Ar$ or petrographic analysis occurs at or near the surface or during subsequent emplacement of thin, rapidly cooled pyroclastic flows. At rhyolitic magma temperatures of $\sim$750°C complete resetting of the K/Ar isotopic system would occur on timescales of a week to years; exsolution lamellae would rapidly undergo homogenization on similar timescales. Extended cooling periods following emplacement of large-volume pyroclastic flows or thick lava flows may also partly to completely reset and texturally homogenize K-feldspars. Due to slow Al–Si diffusion the ordered structural state of basement K-feldspars will be preserved in all cases. Thus, xenocrystic K-feldspar may often be unrecognizable both petrographically and isotopically, but may be identified by X-ray diffraction measurements.

2. Geologic setting

The MPC is located in southern Nevada in the northern McCullough Range (Fig. 1). The southern half of the McCullough Range comprises 1.7 Ga Precambrian monzogranites and gneisses, whereas the northern half exposes Miocene volcanic rocks which lie uncomformably on Precambrian basement.

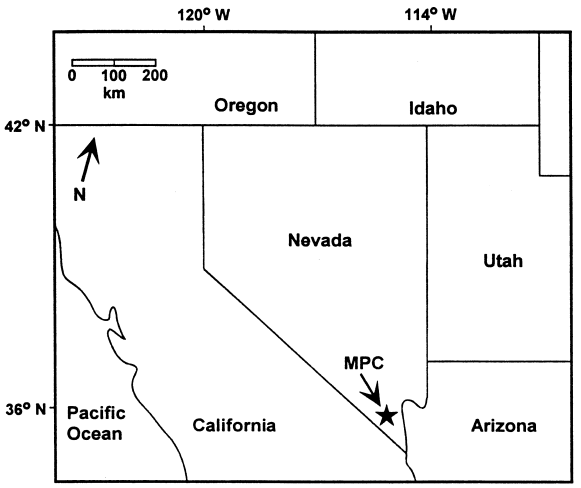

Fig. 1. Map showing location of the MPC.

The MPC is a small caldera with a long dimension of $\sim$2.4 km. Intracaldera units include rhyolite through basalt lava flows and dikes, high-silica rhyolite domes, and volcaniclastic units. The caldera wall exposes the Tuff of Bridge Spring, a welded dacitic ignimbrite, and the underlying Eldorado Valley basalt.

The McCullough Pass Tuff surrounds the MPC except to the east and is composed of three unwelded ignimbrites, each comprising several outflow sheets. Flow units are 3–20 m thick, with estimated volumes of <5 km^3. The tuff is high-silica rhyolite, with a matrix containing phenocrysts of sanidine, plagioclase, biotite and quartz, minor pumice and basalt lithic fragments, with rare granitic lithic fragments and microcline xenocrysts in the two lower ignimbrites. Conglomerates containing clasts of Precambrian basement are found beneath the two lower ignimbrites, whereas the middle and upper ignimbrites are separated by reworked tuff.

3. Analytical methods

Due to the difficulty of retrieving sanidine from the sparse, small pumice in the tuffs whole-rock samples were processed. Ignimbrites and intracaldera domes were processed for mineral separates by crushing, removing rock fragments and visible

alteration, and sieving a 1–2-mm fraction from which sanidine phenocrysts were hand picked. Recovered phenocrysts were treated in dilute HF acid to remove adhering glass. K-feldspar samples from Precambrian rocks were recovered by standard heavy liquid techniques.

$^{40}Ar/^{39}Ar$ analyses were performed in the Nevada Isotope Geochronology Laboratory at the University of Nevada, Las Vegas, NV, USA. Samples were irradiated for 10–14 h at the Texas A&M Nuclear Science Center using Fish Canyon Tuff sanidine, with an age of 27.9 Ma [5,6] as a fluence monitor. Single crystals were loaded into a Cu laser tray and fused with a 20-W CO_2 laser, whereas step-heating analyses used a double vacuum furnace. Argon isotopic analysis was accomplished using a MAP 215-50 rare gas mass spectrometer with a Johnston electron multiplier operated at $\sim 6.0 \times 10^{-17}$ mol mV^{-1} sensitivity. Control of the analysis system and data reduction utilized LabSPEC software written by B. Idleman (Lehigh University).

For single crystal data exhibiting homogeneous age populations analyses outside $\pm 2\sigma$ of the mean were excluded and a weighted mean calculated from the remaining analyses. Inverse variance weighted means used analytical errors with the 0.5% error in J then quadratically combined. For samples with xenocrystic contamination ages for distinct individual populations were calculated in a similar fashion. Crystal populations were also subjected to isochron analysis [7]. Isochrons were initially regressed with all data from a population; if the mean square of weighted deviates (MSWD) was unacceptably high [8] the sample contributing the most to the MSWD was omitted and the isochron regressed again. This process was repeated until an acceptable MSWD was obtained. All analytical errors are reported at the 1σ uncertainty level.

4. Results of $^{40}Ar/^{39}Ar$ dating

Single feldspar crystals from rhyolites were dated by the laser fusion method. A sample of the Tuff of Bridge Springs as well as microcline from Proterozoic granite (step heating) were dated as they represent possible sources of xenocrystic contamination.

Table 1
Summary $^{40}Ar/^{39}Ar$ age data for the MPC

Sample	Unit	Population	$^{40}Ar/^{39}Ar$ Age (Ma ± 1σ)		
		(*n*)	mean	weighted mean	isochron
MPC-19	Capstone Rhyolite	1 (10)	13.93 ± 0.04	13.92 ± 0.08	13.98 ± 0.10[a]
MPC-1	Jean Lake Rhyolite	1 (10)	14.10 ± 0.04	14.10 ± 0.08	14.11 ± 0.12[a]
MPC-43	MPT upper unit	1 (17)	14.07 ± 0.15	14.09 ± 0.08	14.09 ± 0.09[a]
MPC-43	MPT upper unit	2 (3)	14.64 ± 0.11	14.61 ± 0.13[a]	none
MPC-44	MPT middle unit	1 (9)	14.25 ± 0.10	14.23 ± 0.07	14.12 ± 0.13[a]
MPC-44	MPT middle unit	2 (6)	15.12 ± 0.12	15.17 ± 0.08	15.13 ± 0.10[a]
MPC-44	MPT middle unit	3 (6)	1320 ± 380[a]	none	none
MPC-42	MPT lower unit	1 (7)	14.08 ± 0.06	14.09 ± 0.07	14.11 ± 0.12[a]
MPC-42	MPT lower unit	2 (3)	14.65 ± 0.26	14.81 ± 0.08[a]	none
MPC-42	MPT lower unit	3 (6)	1240 ± 160[a]	none	none
Tb-5	TBS	1 (12)	15.01 ± 0.07	15.02 ± 0.08	14.97 ± 0.08[a]
1K-spar	basement	1	893.3 ± 4.1[b]	566–1032[c]	
5K-spar	basement	1	909.5 ± 4.0[b]	383–1194[c]	

MPT, McCullough Pass Tuff; TBS, Tuff of Bridge Springs; *n*, number of crystals in age population; samples and populations within samples arranged in chronostratigraphic order. All analyses are single crystal laser fusion except for 1K-spar and 5K-spar, which are furnace step-heating analyses. For full analytical data see the **Background Dataset** http://www.elsevier.com/locate/epsl

[a]Preferred age.

[b]Total gas age from step-heating analysis.

[c]Range in ages from age spectrum.

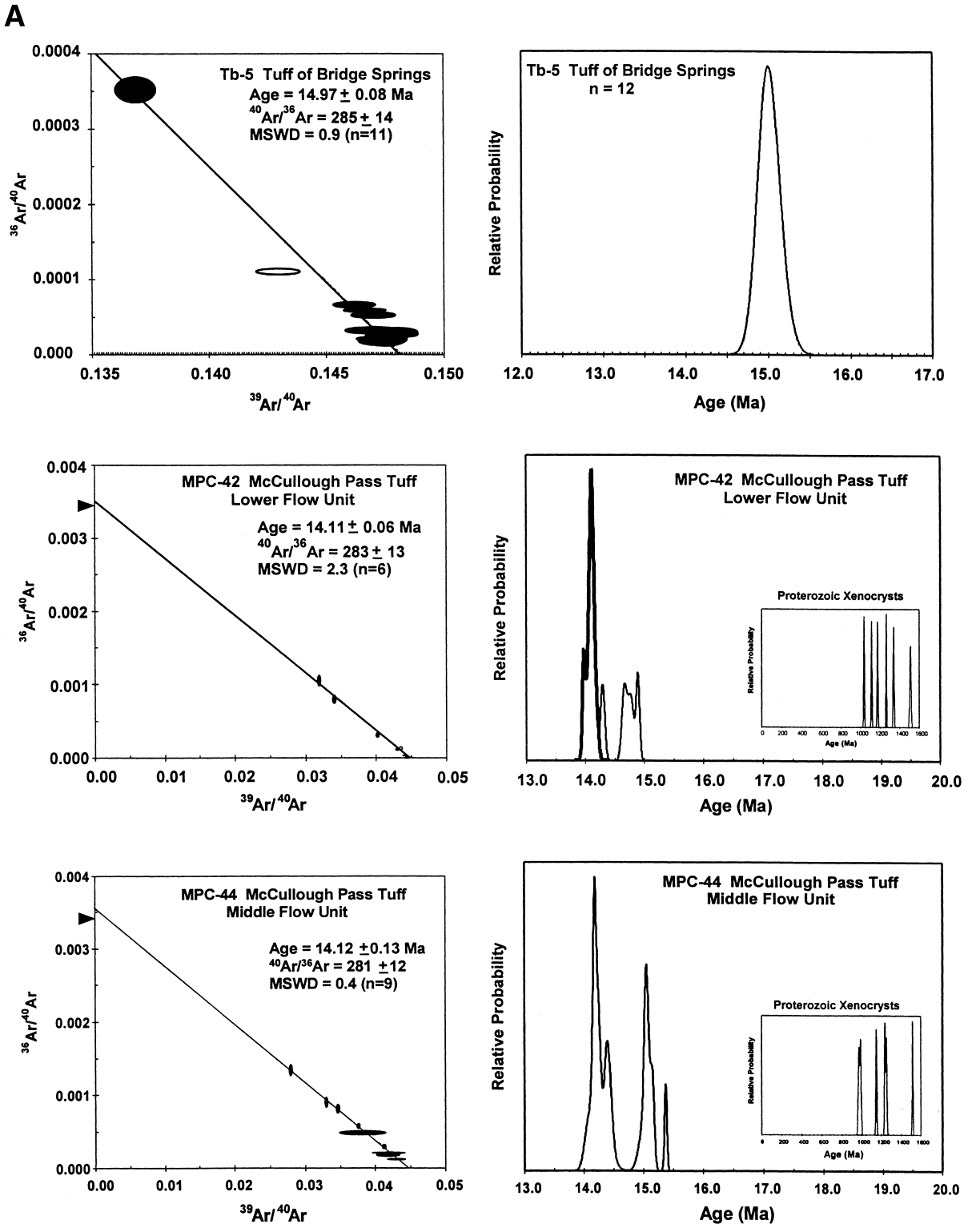
A
Tb-5 Tuff of Bridge Springs
Age = 14.97 ± 0.08 Ma
40Ar/36Ar = 285 ± 14
MSWD = 0.9 (n=11)
36Ar/40Ar
39Ar/40Ar
Tb-5 Tuff of Bridge Springs
n = 12
Relative Probability
Age (Ma)
MPC-42 McCullough Pass Tuff
Lower Flow Unit
Age = 14.11 ± 0.06 Ma
40Ar/36Ar = 283 ± 13
MSWD = 2.3 (n=6)
Proterozoic Xenocrysts
MPC-44 McCullough Pass Tuff
Middle Flow Unit
Age = 14.12 ±0.13 Ma
40Ar/36Ar = 281 ±12
MSWD = 0.4 (n=9)

Fig. 2.

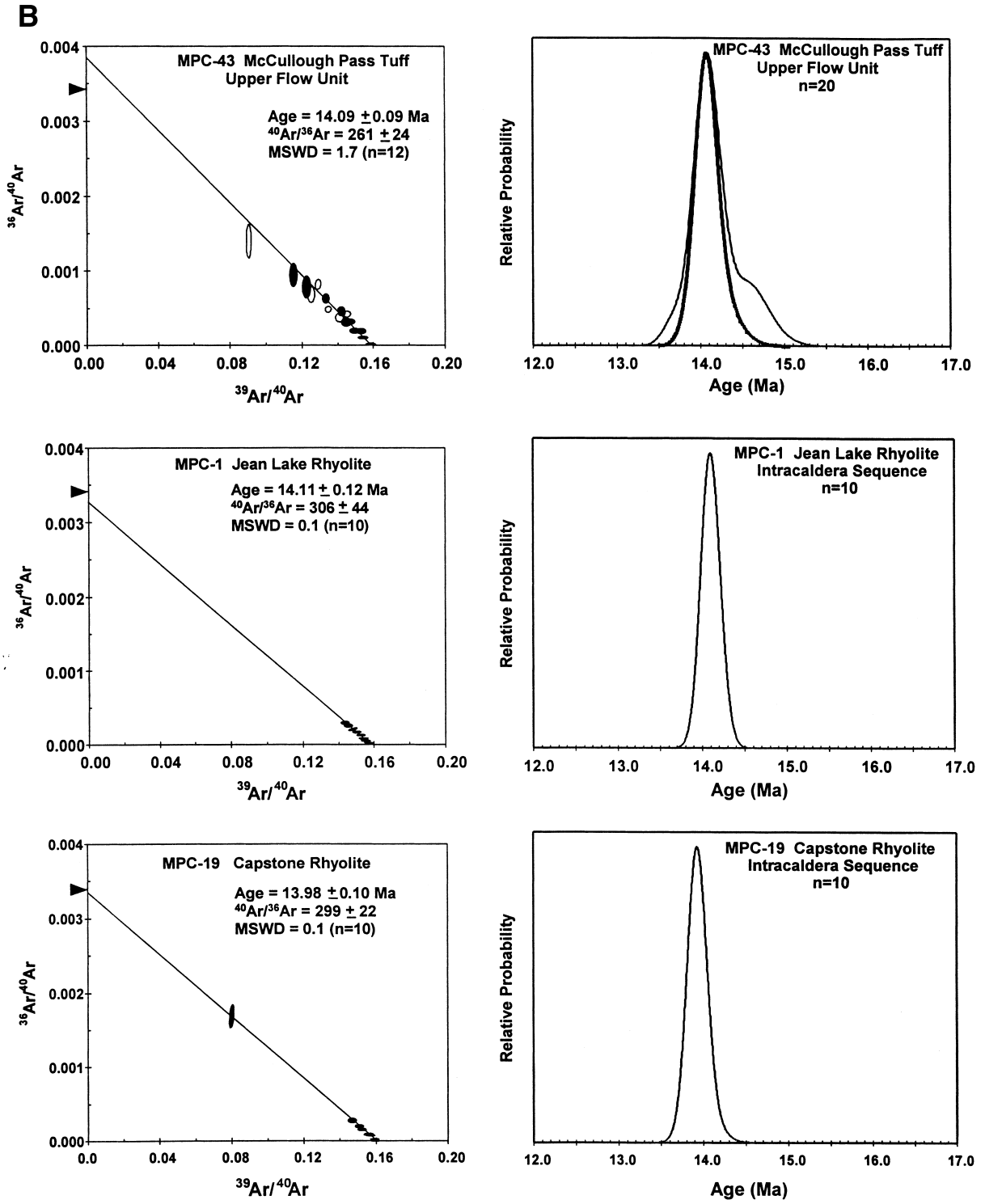

Fig. 2. $^{40}Ar/^{39}Ar$ single crystal isochrons and probability distribution diagrams. Open error ellipses on isochrons indicate omitted data points. Heavy lines on probability distribution curves show trimmed data sets from isochron analysis.

4.1. 1K-spar and 5K-spar, proterozoic basement

Microcline from two samples of Proterozoic granites ~12 km south of the caldera yielded discordant age spectra. Initial ages ranged from ~380–570 Ma rising to Proterozoic ages of 1.0–1.2 Ga with the high-temperature steps (Table 1).

4.2. Tb-5, Tuff of Bridge Springs

The Tuff of Bridge Springs yielded single crystal sanidine ages ranging from 14.91–15.11 Ma ($n=12$) with a mean and standard deviation of 15.01 ± 0.07 Ma (Table 1). All analyses are within $\pm 2\sigma$ and give a weighted mean age of 15.01 ± 0.08 Ma and an isochron age of 14.97 ± 0.08 Ma after omitting one outlier (Fig. 2).

4.3. MPC-42, McCullough Pass Tuff – lower unit

MPC-42, collected from a 7–10-m thick ignimbrite, yielded highly variable ages ($n=16$) from 13.97 Ma to 1.51 Ga (Table 1). There are three populations with mean ages of 14.08 ± 0.06 Ma ($n=7$), 14.77 ± 0.12 Ma ($n=3$), and 1.24 ± 0.16 Ga ($n=6$) (Table 1, Fig. 2). The younger population of juvenile phenocrysts defines an isochron age of 14.11 ± 0.12 Ma after omitting one outlier (Fig. 2).

4.4. MPC-44, McCullough Pass Tuff – middle unit

A sample from this 7–10-m thick ignimbrite yielded variable ages ($n=21$) ranging from 14.08 Ma to 1.52 Ga (Table 1). These analyses define three populations with mean ages of 14.25 ± 0.10 Ma ($n=9$), 15.12 ± 0.12 Ma ($n=6$), and 1.32 ± 0.38 Ga ($n=6$) (Table 1, Fig. 2). The ~15-Ma population yields an isochron age of 15.13 ± 0.10 Ma ($n=6$) and the youngest population ($n=9$) gives an isochron age of 14.12 ± 0.13 Ma (Fig. 2).

4.5. MPC-43, McCullough Pass Tuff – upper unit

A sample from this ~3-m thick ignimbrite yielded ages from 13.67–14.73 Ma ($n=20$) (Table 1). No Proterozoic xenocrysts were found. Three of these analyses yielded ages >14.5 Ma with a mean of 14.64 ± 0.11 Ma. The remainder ($n=17$) define a coherent group with a mean age of 14.07 ± 0.15 Ma (Table 1, Fig. 2) and an isochron age ($n=12$) of 14.09 ± 0.09 Ma (Fig. 2).

4.6. MPC-1, Jean Lake Rhyolite

MPC-1 is from an ~100-m thick lava dome that is stratigraphically near the bottom of the intracaldera sequence. Individual fusions ($n=10$) defined a homogeneous population with ages of 14.06–14.13 Ma (Table 1). All analyses are within 2σ of the mean age of 14.10 ± 0.04 Ma and yield a weighted mean age of 14.10 ± 0.08 Ma and an isochron age of 14.11 ± 0.12 Ma ($n=10$) (Table 1, Fig. 2).

4.7. MPC-19, Capstone Rhyolite

This sample is from an ~100-m thick lava dome that is stratigraphically at the top of the intracaldera sequence. Individual fusions yielded a homogeneous population with ages of 13.85–14.02 Ma (Table 1) and a mean and standard deviation of 13.93 ± 0.04 Ma ($n=10$) (Table 1, Fig. 2). Excluding one analysis outside of $\pm 2\sigma$ yields a weighted mean of 13.92 ± 0.08 Ma. An isochron using all analyses defines an age of 13.98 ± 0.10 Ma (Fig. 2).

5. Discussion

All McCullough Pass Tuff samples exhibit xenocrystic populations with ages of 14.6–15.2 Ma which overlap with those for the Tuff of Bridge Springs (Table 1), suggesting that these ~15-Ma populations were derived from this older unit. That the ~15-Ma populations range to somewhat younger ages suggests that partial resetting of the xenocrysts may have occurred.

The lowermost two units of the McCullough Pass Tuff contain distinct populations of xenocrysts with Proterozoic ages which range from ~1.0 to 1.5 Ga. These ages overlap with those from step-heating analyses of basement feldspars

(Table 1), suggesting that Precambrian xenocrysts were derived from local basement rocks.

5.1. Heat flow and diffusion modelling

5.1.1. Introduction

Coupled heat flow and diffusion modelling was undertaken to place constraints on the timescales and mechanisms involved for incorporation and preservation of xenocrystic K-feldspar in silicic volcanic rocks. Equations for conductive cooling of pyroclastic or lava flows assume an infinite sheet geometry [9] and thermal diffusivity, $\kappa = 1.0$ mm^2/s [10]. Diffusion of Ar, K, and Na in feldspars uses equations for plane sheet (microcline, assuming exsolution lamellae are non-coherent and represent fast diffusion pathways) and spherical (sanidine) geometries [11] and diffusion parameters from Yund [12], Brady [13], Giletti and Shanahan [14], and Lovera et al. [15]. Exact values used for these parameters are given in figure captions.

We consider two initial temperatures; 750°C for rhyolitic magma prior to and during eruption as a lava flow or dome, and 500°C for pyroclastic flows following emplacement. Models simulate xenocrysts incorporated into a magma chamber, into thick (100-m) lava flows, and into thick (50-m) and thin (7-m) pyroclastic flows. Three aspects of the xenocryst problem are assessed; (1) resetting of the K/Ar isotopic system, (2) homogenization of exsolution lamellae, and (3) homogenization of the ordered Al–Si structural state of microcline to the disordered state of sanidine.

5.1.2. Resetting of the K/Ar system – heating in a magma chamber

Models for isothermal heating at 750°C predict complete resetting of the K/Ar isotopic system within a few years to a few decades (Fig. 3) as suggested in other studies [2,16]. Microcline from plutonic or metamorphic rocks, representative of xenocrysts incorporated in a magma chamber at depth, undergoes total loss of argon in 14 days to 3.6 years (Fig. 3). More retentive sanidine is degassed within $\sim$31 years for the largest crystal size modelled (Fig. 3). These timescales are brief compared to the longevity of crustal magma chambers, which may be over 100 ka [17,18], suggesting xenocrysts would be reset before the magma reaches the surface.

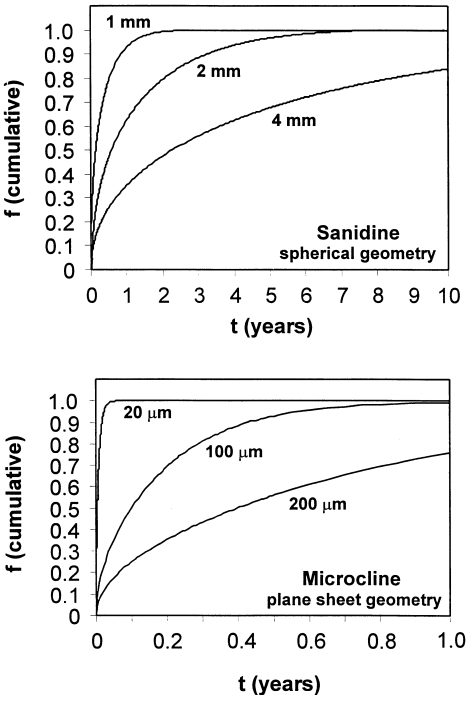

Fig. 3. Fraction argon loss (f) versus time for sanidine and microcline xenocrysts held at a constant temperature of 750°C. Activation energy, $E = 167$ kJ/mol (microcline) and 209 kJ/mol (sanidine); frequency factor $D_0 = 5.5 \times 10^{-4}$ cm^2/s. (microcline) and 2.2 cm^2/s. (sanidine); numbers on lines are diameter or lamellae width. Timescales for complete degassing ($f > 0.99$) are: Sanidine: diameter 1 mm, 1.9 years; diameter 2 mm, 7.7 years; diameter 4 mm, 31 years. Microcline: lamellae width 20 μm, 14 days, width 100 μm, 347 days, width 200 μm, 3.6 years.

5.1.3. Resetting of the K/Ar system – heating in a lava flow/dome

A cooling silicic lava flow or dome was modelled assuming instantaneous emplacement of 750°C magma as a 100-m thick sheet. Large differences in the T–t history exist depending on depth; the surface cools the most rapidly, the base of the flow cools more slowly, and the center of the flow retains heat the longest (Fig. 4A). Thus, the degassing history of xenocrysts will be strongly dependent upon their position within the flow/dome. Temperatures remain isothermal for

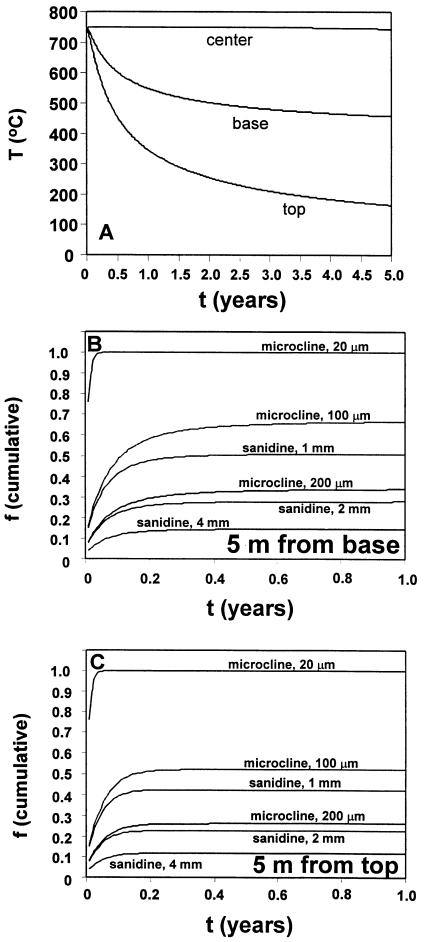

Fig. 4. (A) Cooling curves for a 100-m thick lava flow/dome with an initial emplacement temperature of 750°C. Center, 50 m depth; base, 5 m from base; top, 5 m from top. (B) Fractional argon loss versus time for xenocrysts at base of flow. (C) Fractional argon loss versus time for xenocrysts at top of flow. Diffusion parameters as in Fig. 3.

~3 years at the center of the flow resulting in degassing as for heating in a magma chamber (Fig. 3) except for 4-mm diameter sanidine which reaches a maximum of 80% outgassing.

A position 5 m above the base of the flow cools quickly in the first ~2 years to temperatures of ~500°C (Fig. 4A). This produces complete degassing of microcline with 20-μm width exsolution lamellae in <20 days, however other models do not predict complete resetting (Fig. 4B). For example, microcline with 200-μm width lamellae reaches ~80% degassing, and the most retentive sanidine (4-mm diameter) is only ~55% degassed when diffusion virtually ceases at ~400°C.

Xenocrysts near the surface of the flow experience the most rapid cooling history (Fig. 4A). Microcline with 20-μm width lamellae is totally reset in <20 days, however other xenocrysts are not completely reset (Fig. 4C). For example, microcline with 100-μm lamellae is ~40% reset, whereas the most retentive crystal, 4-mm sanidine, reaches <20% outgassing (Fig. 4C).

5.1.4. *Resetting of the K/Ar system – heating in a pyroclastic flow*

Compared to lava flows, emplacement temperatures of pyroclastic flows may be lower depending on such parameters as height of the eruption column. Welding of ignimbrites requires temperatures of ~575–625°C following emplacement [19]. Unwelded ignimbrites as modelled here are assumed to have emplacement temperatures of 500°C.

We first consider cooling of a 50-m thick ignimbrite. The most significant outgassing is expected near the center of the flow (e.g., Fig. 4). The lower initial temperature and more rapid cooling compared to the lava flow result in only partial resetting; the least retentive microcline xenocryst modelled reaches a maximum of 48% degassing in ~5 years (Fig. 5A). All other models predict <10% outgassing. The fraction Ar loss for xenocrysts near the more rapidly cooled base or surface of the flow would be insignificant; all models predict <2.4% argon loss for these *T–t* histories.

The center of a 7-m thick ignimbrite would cool extremely rapidly compared to other models. This cooling history results in little outgassing, even in the center of the flow (Fig. 5B). All models predict <2% argon loss, with the exception of microcline with 20-μm lamellae which would be degassed ~6.4% (Fig. 5B).

Several factors are not addressed in the models discussed above. The thermal input from latent heat of crystallization would extend the cooling history, especially in the center of thick lava flows and welded ignimbrites, and would thus increase the total amount of degassing and resetting overall. Unwelded or pumice rich ignimbrites have pore spaces which act to decrease the thermal

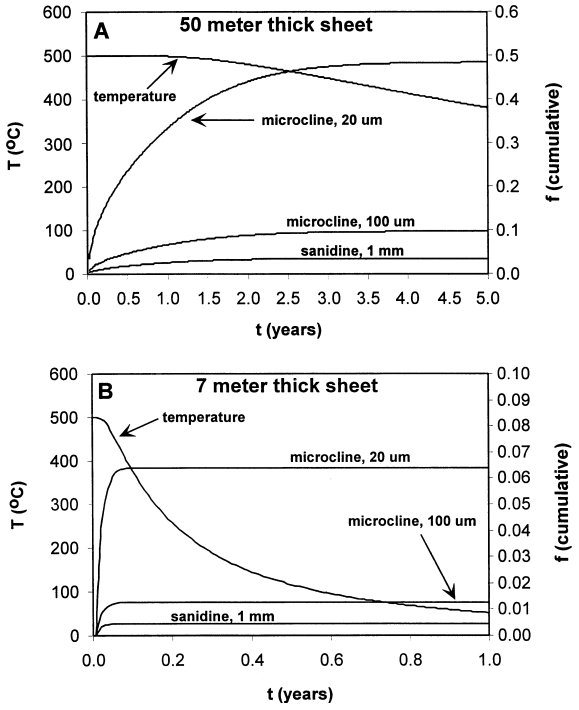

Fig. 5. Cooling histories and corresponding fractional argon loss for ignimbrites with initial emplacement $T = 500$°C. (A) Models for a point at the center of a 50-m thick ignimbrite. (B) Models for a point at the center of a 7-m thick ignimbrite. Diffusion parameters as in Fig. 3.

diffusivity and extend the cooling history. However, a potential opposing effect is more rapid cooling induced by fractures or gas advection through permeable ignimbrites. Thus, in general the models presented here should represent a good approximation to xenocryst degassing behavior.

5.1.5. *Homogenization of exsolution lamellae*

Given sufficient temperature and time, exsolution lamellae in orthoclase or microcline will undergo homogenization, making low-temperature basement feldspars unidentifiable petrographically. Models assume that exsolution lamellae are non-coherent and exhibit perfect unmixing, i.e., adjacent lamellae are pure albite and pure orthoclase end members. These models thus predict a maximum homogenization time as natural samples may not be perfectly unmixed. Complete homogenization is assumed when the dimensionless diffusion parameter $Dt/r^2 > 0.5$, at which point $< 1\%$ of the original compositional difference between adjacent lamellae remains [11].

Models for heating in a magma chamber at 750°C yield results similar to those for resetting of the K/Ar system (Fig. 3). Feldspars with 20–200-μm width lamellae undergo complete homogenization in 47 days to 18.7 years (Fig. 6A). Slow cooling in the center of a 100-m lava flow emplaced at 750°C (Fig. 4A) yields identical results with the exception of models for 200-μm width lamellae, which reaches only 66% homogenization. Models for a point 5 m above the base of the flow predict feldspars with 20-, 100-, and 200-μm width lamellae reach 84, 17, and 8% homogenization (Fig. 6B) when diffusion ceases at ~ 550°C. Similar results are predicted for a position near the top of the flow.

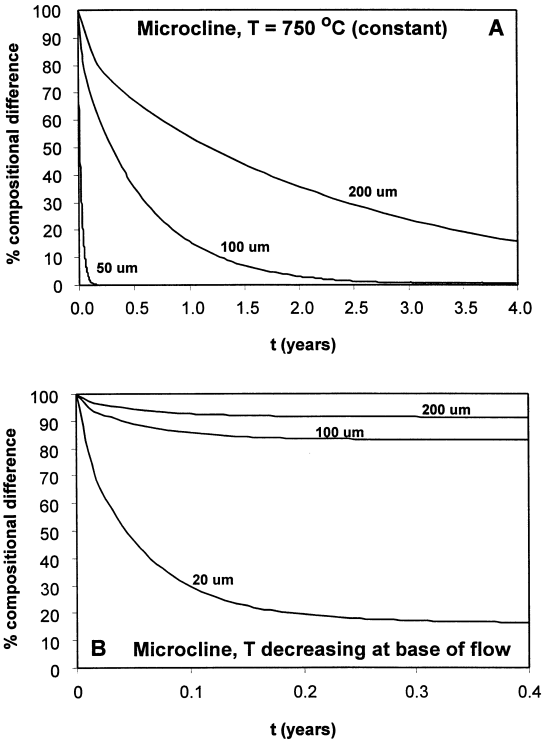

Fig. 6. Diffusional homogenization modelling of exsolution lamellae in microcline. Models use activation energy, $E = 280$ kJ/mol; frequency factor, $D_0 = 16$ cm^2/s. (A) Models for a subvolcanic magma chamber at a constant temperature of 750°C. (B) Models for the base of a 100-m thick lava flow emplaced at 750°C.

It is apparent from the above that no significant homogenization of exsolution lamellae would be expected for xenocrysts in ignimbrites emplaced at temperatures of ~500°C. In contrast, annealing for sufficient time at subsolvus temperatures of ~400–600°C induces growth of exsolution lamellae at the nm scale of cryptoperthites (e.g., [12]). Thus, little change in the appearance of μm-scale lamellae as modelled here would occur.

5.1.6. Disordering of the Al–Si tetrahedral siting

Data for Al–Si exchange during disordering of microcline to sanidine indicate significantly lower diffusion rates than those for Ar, K, or Na, with most activation energies in the range of 350–420 kJ/mol [13,20]. Laboratory studies typically utilize temperatures of 1000–1100°C to induce disordering of Al–Si siting in feldspars [20–22]. Lower temperatures (e.g., 750°C for 28 days) have been found to have no measurable effect [22]. The phase transformation from microcline to sanidine in metamorphic rocks occurs at ~500°C on timescales of regional metamorphism spanning millions of years [23]. Sipling and Yund [20] estimate that 20–100 Ma are required for disordering at 600°C. The extremely brief timescales which xenocrysts may be exposed to such temperatures in our models suggests no significant disordering would occur. Thus, xenocrysts which have been completely outgassed of pre-existing argon as well as having undergone homogenization of exsolution lamellae may still be identifiable by their ordered Al–Si tetrahedral siting.

5.2. Implications of models for xenocrysts in the McCullough Pass Tuff

Xenocrysts in the lowermost two flow units of the McCullough Pass Tuff represent material from Proterozoic basement rocks (microcline) and the 15-Ma Tuff of Bridge Springs (sanidine) exposed in the caldera wall. These xenocrysts were incorporated either within the subvolcanic magma chamber prior to eruption, during propagation of the magma to the surface, or during emplacement of the pyroclastic flows. All three possibilities exist for the Proterozoic xenocrysts; only the final two are likely for the ~15-Ma xenocrysts.

Crystals may remain suspended in viscous rhyolitic magmas for periods as long as 100 ka prior to eruption [17,18]. It is thus unlikely that xenocrystic microcline with Proterozoic ages was incorporated into the magma chamber prior to eruption as complete resetting of the K/Ar system would occur within weeks to a few years (Fig. 3). Thus, xenocrysts were likely incorporated during magma transport to the surface, or upon emplacement of pyroclastic flows. This would result in essentially the same thermal history for the xenocrysts; rapid heating followed by cooling at the surface in the flow.

Spatial variations in lithic clast components of ignimbrites often reflect incorporation of locally exposed alluvium (e.g. [24]). The correlation of conglomerates containing Proterozoic clasts beneath the two lower ignimbrite units (MPC-42 and MPC-44) with the presence of Proterozoic K-feldspar xenocrysts in these units suggests contamination occurred during emplacement of the pyroclastic flows. The relatively low emplacement temperatures and rapid cooling rates of small volume, unwelded ignimbrites would allow such xenocrysts to retain >93% of their pre-existing argon (Fig. 5). The discrete age populations which are preserved are consistent with this prediction (Table 1). The lack of Proterozoic material in the uppermost ignimbrite (MPC-43) further argues for incorporation of xenocrysts during emplacement of the pyroclastic flows. The underlying ignimbrites blanket the paleosurface over which the upper flow was emplaced, thus isolating the upper ignimbrite from Proterozoic material during emplacement.

The ~15-Ma xenocryst populations present in all three tuffs exhibit ages which overlap with those measured for the Tuff of Bridge Springs, but which range down to 14.6 Ma (Table 1). The younger ages could be due to small amounts of radiogenic argon loss from xenocrysts following emplacement. For example, a 15-Ma crystal which undergoes 1.4% argon loss will be reduced in apparent age from 15.0 to 14.6 Ma. This is in agreement with the small amounts of degassing predicted for thin, low-volume ignimbrites such as these.

Samples from the Jean Lake Rhyolite and Cap-

stone Rhyolite domes lacked identifiable xenocrystic contamination (Table 1). This is consistent with models presented above which indicate that, especially in the more central parts of such units, complete resetting of xenocrysts may occur. Incorporation of foreign material at the surface may also be less likely in a slowly advancing lava flow or dome compared to an explosively erupted ignimbrite. Thus, xenocrysts, if present, may be more commonly incorporated prior to eruption with an increased exposure time to magmatic temperatures.

5.3. Other examples and implications

The models presented here predict that xenocrystic contamination would be more apparent in rapidly cooled distal pyroclastic deposits, near the base or top of large ignimbrites and lava flows, the carapace breccias of domes and flows, thin lava flows or ignimbrites, and pyroclastic air fall units. An increased occurrence of contamination might also be apparent in explosively versus effusively erupted rocks.

Numerous examples that conform to these expectations have been revealed by laser fusion $^{40}Ar/^{39}Ar$ dating. Mixed juvenile and xenocrystic feldspar populations were documented in the Huttenberg tephra, a small volume phonolite unit in the East Eifel Volcanic Field of Germany [25]. Dating of the Laacher See Tephra, another small volume (~ 5 km^3) unit in the East Eifel Volcanic Field, indicated that $\sim 20\%$ of analyzed crystals were xenocrysts [4]. Xenocrystic contamination of a small volume 580-ka trachyte pumice flow with basement feldspars up to 330 Ma was documented by LoBello et al. [3]. Most of these examples would have had post-emplacement cooling histories similar to those calculated for the McCullough Pass Tuff (Fig. 5B). Sanidine phenocryst ages from rhyolite domes at Mono Craters, California, showed no significant xenocrystic contamination [26]. In contrast, heavily contaminated crystal populations were found in tephra layers produced in initial explosive phases of the same eruptions [27]. In studies of Yellowstone volcanic field rhyolites, large-volume ignimbrites generally showed greater degrees of xenocrystic contamination than lava flows [16]. Analyses of sanidine from lava domes and flows of the Taylor Creek Rhyolite, southwestern New Mexico, yielded highly reproducible ages with no evidence of xenocrysts [1]. In these cases preservation of xenocrysts is likely due to the cooler emplacement temperatures of pyroclastic flows or tephra deposits. These examples show that the occurrence of detectable xenocrystic contamination is more common in explosively erupted and thin deposits emplaced at lower temperatures, however it is apparent that regardless of the size and emplacement temperature of the eruptive unit, more quickly cooled parts (e.g., edges of flows) are more likely to preserve detectable xenocrysts.

Some models invoke incorporation of xenocrysts into the subvolcanic magma chamber prior to eruption. Suggested mechanisms include scavenging of the crystallized magma chamber margin (i.e., cognate material) [28], or incorporation of material from previously solidified magma bodies [4]. Active volcanic systems with pluton emplacement on intervals of 72–12 ka [4] would have highly elevated geotherms, as timescales for thermal relaxation following pluton emplacement are of similar, or longer, intervals [18]. Thus, temperatures may be as high as ~ 500°C at pre-eruptive silicic magma chamber depths of ~ 6 km, especially near active magma reservoirs. Xenocrysts with ages hundreds of thousands of years older than eruptive ages would have been maintained at such elevated temperatures for hundreds of thousands of years. Under such conditions sanidines with 1–4-mm diameters are $> 99\%$ outgassed after 8–120 ka, respectively. Microclines are totally outgassed in < 10 ka. Thus, severe restrictions are placed on derivation of detectable xenocrystic material from this environment; ambient temperatures must be relatively low and xenocrysts must be incorporated into the magma very near to the time of its transport to the surface [28]. In general we suggest xenocrysts with significantly older ages than juvenile phenocrysts are not likely to be derived from plutonic levels.

The predicted rapid loss of pre-existing argon and homogenization of exsolution lamellae for feldspars incorporated into a silicic magma chamber suggests that most detectable xenocrystic con-

tamination occurs at, or near the surface. Fragmentation of wall rock during propagation of magma to the surface provides an easily identifiable mechanism, as does erosion of the vent and incorporation of alluvial material during emplacement of flows. Data presented here argue for incorporation of lithic clasts and xenocrysts during emplacement of the McCullough Pass Tuff on the paleosurface. A similar conclusion has been reached for other ignimbrites, e.g., the Peach Springs Tuff [29] and the Bishop Tuff [24]. The presence of detectable xenocrystic K-feldspars in pumice clasts, however, demands incorporation into the magma prior to vesiculation and eruption; we suggest such contamination occurs during movement of magma towards the surface, not at plutonic depths. Xenocrysts present in rhyolite flows and pumice in the Yellowstone Volcanic Field are attributed to incorporation of wall rock during movement of the magmas to the surface [16]. Consistent with our conclusions, $^{40}Ar/^{39}Ar$ analyses showed that more contamination was apparent in tuffs, which was attributed to further degassing of xenocrysts during extended cooling of the lava flows [16].

The models presented suggest that well-designed sampling strategies may minimize the problems presented by the presence of xenocrysts. Samples from the central parts of thick rhyolitic domes, lavas or thick, welded ignimbrite sheets are more likely to preserve a homogeneous age population of crystals, regardless of the origin of those crystals as juvenile phenocrysts, cognate material, or xenocrysts. Lavas and large ignimbrites may initially preserve xenocrysts at the edges, but with time these edges may be eroded away, exposing parts of the flow/ignimbrite which experienced a more extended cooling history and thus greater degrees of resetting of any xenocrysts that may have been present.

6. Summary

Small volume ignimbrites at MPC preserve evidence for significant contamination by xenocrystic K-feldspars derived from a stratigraphically lower ignimbrite as well as Proterozoic basement. In contrast, crystal populations from thick lava domes yield homogeneous eruptive ages, with no evidence for xenocrystic contamination. Xenocrysts in the ignimbrites were preserved due to being incorporated into magmas near, or at the surface, and experiencing little reheating on rapid cooling of the thin outflow sheets. Despite severe contamination $^{40}Ar/^{39}Ar$ dating provides reliable eruption ages for all units at $\sim$14 Ma.

Xenocrystic feldspars may be recognized petrographically, structurally (i.e., X-ray diffraction) and isotopically. If incorporated into a subvolcanic magma chamber at $\sim$750°C, low-temperature basement K-feldspars would undergo homogenization of exsolution lamellae and be totally outgassed of previously accumulated radiogenic argon within a few years, making them petrographically and isotopically indistinguishable from juvenile sanidine phenocrysts. However, such xenocrysts may still be chemically and structurally distinct, e.g., retaining the ordered Al–Si tetrahedral siting of low-temperature feldspars. Effusive eruptions of silicic magma typically form lava domes or flows which may be hundreds of meters thick and ignimbrites with similar thicknesses and initial temperatures in flow interiors near magmatic values. Temperatures may remain significantly elevated for periods of time ranging into decades. Thus, partial, or complete resetting of the argon isotopic system may also occur during cooling in thick rhyolite domes, flows and large ignimbrites, although the possibility of preservation of exsolution lamellae and anomalously old ages is significantly higher, especially for crystals near the edges of these units where cooling is relatively rapid. In contrast, post-emplacement cooling in thin, non-welded pyroclastic flows ($<$10 m) may be rapid enough that complete preservation of low-temperature feldspar textures retention of inherited Ar isotopic systematics may often occur.

Acknowledgements

We thank Oscar Lovera (UCLA) for assistance with diffusion modelling and Easte Warnick (UNLV) for work on mineral separates. The

Nevada Isotope Geochronology Laboratory was funded by NSF Grant EPS-9720162 to T.S.*[RV]*

References

[1] W.A. Duffield, G.B. Dalrymple, The Taylor Creek Rhyolite of New Mexico: a rapidly emplaced field of lava domes and flows, Bull. Volcanol. 52 (1990) 475–487.

[2] T.L. Spell, T.M. Harrison, $^{40}Ar/^{39}Ar$ geochronology of post-Valles Caldera rhyolites, Jemez Mountains volcanic field, New Mexico, J. Geophys. Res. 98 (1993) 8031–8051.

[3] Ph. Lo Bello, G. Feraud, C.M. Hall, D. York, P. Lavina, M. Bernat, $^{40}Ar/^{39}Ar$ step-heating and laser fusion dating of a Quaternary pumice from Neschers, Massif Central, France: The defeat of xenocrystic contamination, Isot. Geosci. 66 (1987) 61–71.

[4] P. van den Bogaard, $^{40}Ar/^{39}Ar$ ages of sanidine phenocrysts from Laacher See Tephra (12,900 yr BP): Chronostratigraphic and petrologic significance, Earth Planet. Sci. Lett. 133 (1995) 163–174.

[5] T.A. Steven, H.H. Mehnert, J.D. Obradovich, Age of volcanic activity in the San Juan Mountains, Colorado, US Geol. Surv. Prof. Pap. 575-D (1967) 47–55.

[6] G.T. Cebula, M.J. Kunk, H.H. Mehnert, C.W. Naeser, J.D. Obradovich, J.F. Sutter, The Fish Canyon Tuff, a potential standard for the ^{40}Ar-^{39}Ar and fission-track dating methods (abstract), Terr. Cogn. (6th Int. Conf. Geochronol. Cosmochronol. Isot. Geol.) 6 (1986) 139.

[7] D. York, Least squares fitting of a straight line with correlated errors, Earth Planet. Sci. Lett. 5 (1969) 320–324.

[8] I. Wendt, C. Carl, The statistical distribution of the mean squared weighted deviation, Chem. Geol. 86 (1991) 275–285.

[9] H.S. Carslaw, J.C. Jaeger, Conduction of Heat in Solids, 2nd edn., Oxford University Press, Oxford, 1988, 510 pp.

[10] W.B. Durham, V.V. Mirkovich, H.C. Heard, Thermal diffusivity of igneous rocks at elevated pressure and temperature, J. Geophys. Res. 92 (1987) 11615–11634.

[11] J. Crank, The Mathematics of Diffusion, 2nd edn., Oxford University Press, Oxford, 1975, 414 pp.

[12] R.A. Yund, Microstructure, kinetics, and mechanisms of alkali feldspar exsolution, in: P.H. Ribbe (Ed.), Feldspar Mineralogy, Reviews in Mineralogy, Volume 2, 2nd edn., 1983, pp. 177–202.

[13] J.B. Brady, Diffusion data for silicate minerals, glasses, and liquids, in: T.J. Ahrens (Ed.), Mineral Physics and Crystallography, A Handbook of Physical Constants, AGU Reference Shelf 2, 1995, pp. 269–290.

[14] B.J. Giletti, T.M. Shanahan, Alkali diffusion in plagioclase feldspar, Isot. Geosci. 139 (1997) 3–20.

[15] O.M. Lovera, M. Grove, T.M. Harrison, K.I. Mahon, Systematic analysis of K-feldspar $^{40}Ar/^{39}Ar$ step heating results: I. Significance of activation energy determinations, Geochim. Cosmochim. Acta 61 (1997) 3171–3192.

[16] C.A. Gansecki, G.A. Mahood, M. McWilliams, $^{40}Ar/^{39}Ar$ geochronology of rhyolites erupted following collapse of the Yellowstone caldera, Yellowstone Plateau volcanic field: implications for crustal contamination, Earth Planet. Sci. Lett. 142 (1996) 91–107.

[17] M.R. Reid, C.D. Coath, M. Harrison, K.D. McKeegan, Prolonged residence times for the youngest rhyolites associated with Long Valley Caldera: ^{230}Th–^{238}U ion microprobe dating of young zircons, Earth Planet. Sci. Lett. 150 (1997) 27–39.

[18] C.J. Hawkesworth, S. Blake, P. Evans, R. Hughes, R. Macdonald, L.E. Thomas, S.P. Turner, G. Zellmer, Time scales of crystal fractionation in magma chambers – Integrating physical, isotopic and geochemical perspectives, Earth Planet. Sci. Lett. 41 (2000) 991–1006.

[19] J.R. Reihle, Calculated compaction profiles of rhyolitic ash-flow tuffs, Geol. Soc. Am. Bull. 84 (1973) 2193–2216.

[20] P.J. Sipling, R.A. Yund, Kinetics of Al/Si disordering in alkali feldspars, in: A.W. Hofmann, B.J. Giletti, H.S. Yoder Jr., R.A. Yund, (Eds.), Geochemical Transport and Kinetics, Carnegie Institute of Washington and Academic Press, New York, 1974, pp. 185–193.

[21] S.A. Hayward, E.K.H. Salje, Displacive phase transition in anorthoclase: The 'plateau effect' and the effect of T1–T2 ordering on the transition temperature, Am. Mineral. 81 (1996) 1332–1336.

[22] D. Nyfeler, T. Armbruster, I.M. Villa, Si, Al, Fe order-disorder in Fe-bearing K-feldspar from Madagascar and its implications to Ar diffusion, Schweiz. Mineral. Petrogr. 78 (1998) 11–20.

[23] W.H. Bernotat, G. Morteani, The microcline/sanidine phase transformation isograd in metamorphic regions: Western Tauern Window and Merano–Mules–Anterselva complex (Eastern Alps), Am. Mineral. 67 (1982) 43–53.

[24] C.J.N. Wilson, W. Hildreth, The Bishop Tuff: New insights from eruptive stratigraphy, J. Geol. 105 (1997) 407–439.

[25] P. van den Bogaard, C.M. Hall, H.-U. Schnimcke, D. York, Precise single-grain $^{40}Ar/^{39}Ar$ dating of a cold to warm climate transition in Central Europe, Nature 342 (1989) 523–525.

[26] Q. Hu, P.E. Smith, N.M. Evensen, D. York, Lasing in the Holocene: extending the $^{40}Ar/^{39}Ar$ laser probe method into the ^{14}C range, Earth Planet. Sci. Lett. 123 (1994) 331–336.

[27] Y. Chen, P.E. Smith, N.M. Evensen, D. York, K.R. Lajoie, The edge of time dating young volcanic ash layers with the $^{40}Ar/^{39}Ar$ laser probe, Science 274 (1996) 1176–1178.

[28] C.A. Gansecki, G.A. Mahood, M. McWilliams, New ages for the climactic eruptions at Yellowstone Single-crystal $^{40}Ar/^{39}Ar$ dating identifies contamination, Geology 26 (1998) 343–346.

[29] J.E. Nielson, D.R. Lux, G.B. Dalrymple, A.F. Glazner, Age of the Peach Springs Tuff, southeastern California and western Arizona, J. Geophys. Res. 95 (1990) 571–580.